Bioorganic Chemistry 110 (2021) 104770

Contents lists available at ScienceDirect

Bioorganic Chemistry

journal homepage: www.elsevier.com/locate/bioorg

Design, synthesis and evaluation of dihydropyranoindole derivatives as potential cholinesterase inhibitors against Alzheimer's disease

Sarfaraz Shaikh [a], Ganesh Pavale [a], Pratik Dhavan [b], Pinky Singh [c], Jasmin Uparkar [a], S. P. Vaidya [c], B.L. Jadhav [b], M.M.V. Ramana [a,*]

[a] Department of Chemistry, University of Mumbai, Santacruz (E), Mumbai 400 098, India
[b] Department of Life Sciences, University of Mumbai, Santacruz (E), Mumbai 400 098, India
[c] Department of Microbiology, Haffkine Institute, Parel, Mumbai 400012, India

ARTICLE INFO

Keywords:
Cholinesterase inhibitor
Cell viability
DNA damage
Antioxidant
Molecular docking

ABSTRACT

A series of novel dihydropyranoindole derivatives containing sulphonamide group were designed, synthesized and evaluated for *in-vitro* anti-cholinesterase activity. The result showed that all the compounds exhibited potent acetylcholinesterase (AChE) activity (IC_{50} = 0.41–8.79 μM) while demonstrated moderate to good activity for butyrylcholinesterase (BuChE) (IC_{50} = 1.17–30.17 μM). The tested compounds exhibited selectivity towards AChE over BuChE. Compound **5o** was most potent towards both AChE (IC_{50} = 0.41 μM) and BuChE (IC_{50} = 1.17 μM) when compared to standard galantamine and rivastigmine. Enzyme kinetics and molecular docking studies revealed that compound **5o** shows mixed type inhibition and binds to peripheral anionic site (PAS) and the catalytic sites (CAS) of both the enzymes. Furthermore, cell viability studies were also performed against N2a cells along with neuroprotection studies against H_2O_2 in the same cell line. Antioxidant studies using DPPH radical and H_2O_2 were also performed which revealed that all compounds possessed some antioxidant activity. Also, DNA damage protection assay for compound **5o** was performed implying that compound **5o** was protective in nature. ADME studies were also performed which demonstrated good pharmacokinetics. These findings indicated that dihydropyranoindole derivatives could be possible drug lead in the search for new multifunctional AD drugs.

1. Introduction

Alzheimer's disease (AD) is progressive neurodegenerative brain disorder that is jeopardizing the health of elderly population. AD is characterized by dementia, memory loss and irreversible cognitive impairment which inevitably lead to intellectual disability [1]. It affects nearly 40 million people worldwide and it is predicted to be more than 131 million by 2050 [2]. Although the etiology of AD is unclear and complicated, a number of hypotheses have been proposed like low acetylcholine levels, β-amyloid (Aβ) peptides agglomeration, hypoxia, oxidative stress and τ-protein hyperphosphorylation [3,4]. Available AD drugs such as donepezil, rivastigmine and galantamine provide symptomatic improvement by increasing the acetylcholine levels and inhibiting acetylcholinesterase (AChE) but also impart several side effects such as periphery side effect, hepatotoxicity and gastrointestinal tract disorders [4,5]. Hence, there is an urge to identify and develop novel efficacious pharmacophores and curtail the toxicity that can treat the underlying cause of AD.

The crystal structure of AChE (PDB ID: 1EVE) possesses two primary binding sites i.e. a catalytic active site (CAS) at the bottom of the deep narrow gorge, and a peripheral anionic site (PAS) near the gorge entrance [6]. CAS acts as a binding site for substrates and inhibitors and comprises of three amino acid residues Ser200, His440 and Glu327 while PAS is the binding site for the enzyme inhibitor consisting of Tyr70, Asp72, Tyr121, Trp279, Phe290 and Tyr334 residues [7]. PAS also induces the formation of Aβ-amyloid aggregates and accelerates Aβ-amyloid deposition [8]. Taking these findings into account, it is must to design dual-site AChE inhibitor that should be capable of interacting with both CAS and PAS sites simultaneously.

In the area of drug discovery, indole is a versatile heterocyclic nucleus finding applications in medicinal chemistry. Owing to its privileged structure, indole moiety exhibits various pharmacological activities such as anti-inflammatory [9], antimicrobial [10], antioxidant [11], anti-tubercular [12], antihistaminic [13] anticancer [14] and

* Corresponding author.
E-mail address: mmvramana@yahoo.co.in (M.M.V. Ramana).

https://doi.org/10.1016/j.bioorg.2021.104770
Received 24 November 2020; Received in revised form 29 January 2021; Accepted 21 February 2021
Available online 23 February 2021

Alzheimer agent [15]. Also, indole can bind to multiple receptors with high affinity like 5-lipoxygenase inhibitors [16], selective dopamine agonist [17] and steroid 5α-reductase inhibitor [18]. Atevirdine, indomethacin, indolequinone and delavirdine are several marketed drugs that bear indole moiety. Some naturally occurring indole derivatives are tryptophan (amino acid), serotonin (neurotransmitter) and psilocybin (psychotic) [19]. On the other hand, 4H-chromene find diverse range of biological activities such as antimicrobial [20], antiviral [21], antioxidant [22], acetylcholinesterase inhibitors [22] and several other interesting biomedical applications. Similar to indole and 4H-chromene, sulphonamides analogues find a variety of applications in treatment of different diseases such as antimicrobial [23], anti-inflammatory [24], antidiabetic [25] and acetylcholinesterase inhibitory agents [26].

There are many reports on AD using indole, for e.g. López-Iglesias et al. [27] reported melatonin derived Alzheimer's drugs, Więckowska et al. [28] reported 1-(phenylsulfonyl)-4-(piperazin-1-yl)-1H-indole as multi-target-directed ligands for AD and Ghanei-Nasab et al. [29] reported coumarin-3-carboxamides bearing tryptamine moiety. Similarly, Kumar et al. [30] designed 2-amino-4H-pyrans as potent cholinesterase inhibitors while Boulebd et al. [31] reported imidazopyranotacrines as selective acetylcholinesterase inhibitors. Sulphonamide derivatives were reported by Swetha et al. [32] and Masand et al. [26] as potential Alzheimer agents. Prompted from these reports and the biological significance of indole, 4H-chromene and sulphonamide it is reasonable to conclude that fusion of these moieties may lead to increased activity (Fig. 1).

In the present study, we designed and synthesized a series of novel dihydropyranoindole derivatives using ultrasonication. The newly synthesized derivatives were pharmacologically evaluated for their *in-vitro* cholinesterase inhibition, enzyme kinetic inhibition, *in-vitro* cell viability using N2a cells and cytoprotective effect against H_2O_2 using N2a cells. In addition, DNA damage protection against Fenton's reagent was performed. Moreover, docking studies of the synthesized derivatives were carried out computationally and were subjected to *in silico* ADME prediction in order to understand their pharmacokinetic behaviour.

2. Results and discussion

2.1. Chemistry

The route for the synthesis dihydropyranoindole derivatives **5 (a-o)** is outlined in Scheme 1. In the first step 1-tosyl-1H-indol-4-ol (**2**) was prepared by reacting 4-Hydroxyindole (**1**) and Tosyl chloride in presence of ^{t}BuOK at 0 °C for 45 min according to the published procedure [33]. Later the tosylated product (**2**) was reacted with substituted aldehyde **3 (a-o)** and malononitrile (**4**) in the presence of triethylamine in ethanol at 80 °C to obtain dihydropyranoindole derivatives **5 (a-o)**. The final product was purified by crystallization using methanol in good to excellent yield.

The synthesized dihydropyranoindole derivatives were successfully characterized by spectral (IR, ^{1}H NMR, ^{13}C NMR, MS) and elemental analyses. The FT-IR spectrum of the synthesized compound showed sharp absorption band in the range of 3300 cm^{-1} which can be assigned to NH_2 stretching. Also a sharp band around 2200 cm^{-1} can be assigned to nitrile group whereas a band at 1185 cm^{-1} can be ascribed to SO_2 group. ^{1}H NMR spectrum displayed the proton around δ = 4.7 ppm corresponding to the methine (CH) proton of the pyran ring. In ^{13}C NMR spectrum, a peak around δ = 109 ppm for nitrile group and a peak at δ = 56 ppm for methine carbon of the pyran ring confirms the product formation.

2.2. Biology

2.2.1. In-vitro cholinesterase activity

Synthesized compounds **5 (a-o)** were accessed for their potential AChE/BuChE inhibitory properties according to modified Ellman's method [34]. Galantamine and rivastigmine were used as reference drugs. The results are summarized in Table 1. The IC_{50} values of tested compounds ranged between 0.41 and 8.79 μM for AChE and 1.17 to 30.17 μM for BuChE suggesting that tested compounds exhibited higher inhibitory activity against AChE. A total of eight derivatives exhibited improved AChE activity than the standard drugs, although only one derivative exhibited better BuChE activity when compared to standards.

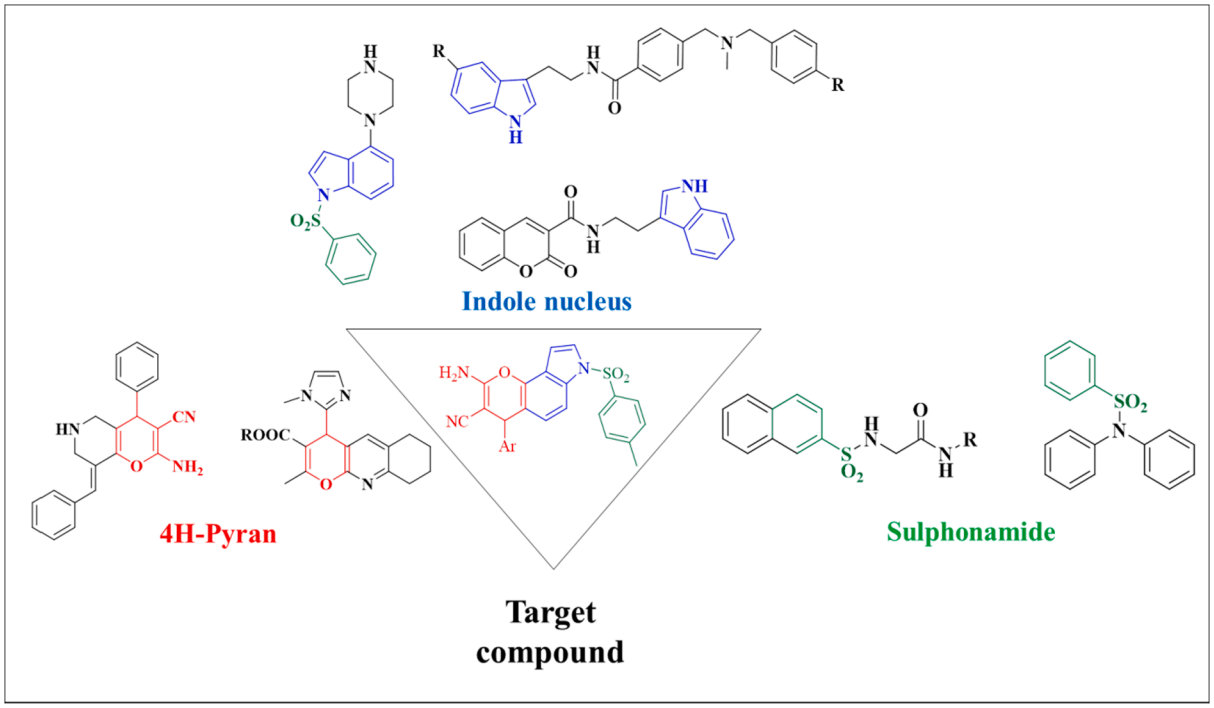

Fig. 1. Design strategy for target compound.

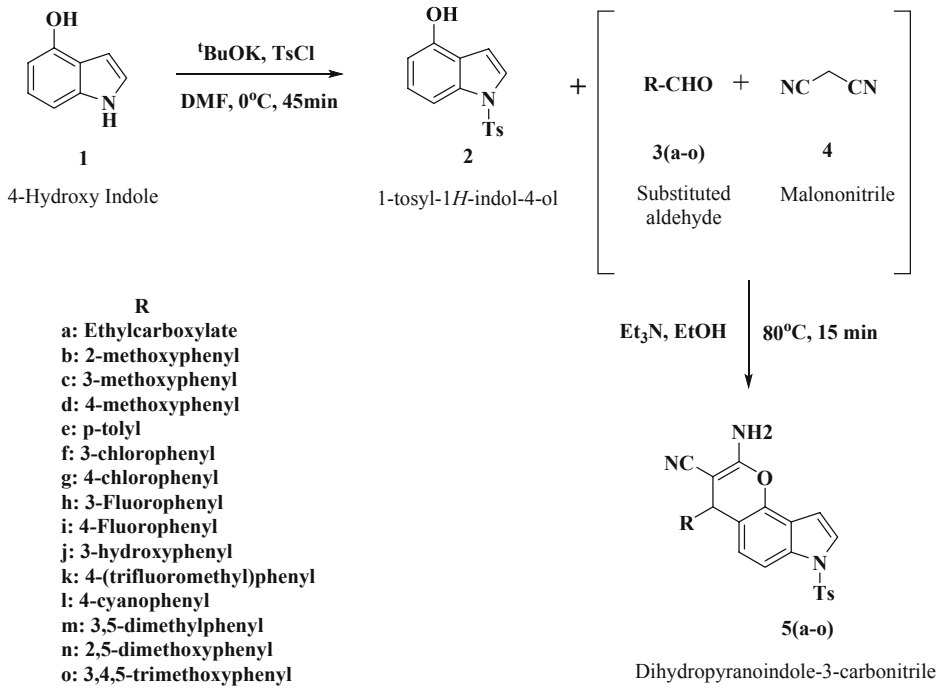

Scheme 1. Synthesis of novel dihydropyranoindole.

Compound **5o** exhibited the highest inhibition value (IC_{50} = 0.41 ± 0.16 μM) in comparison to the standard drugs galantamine (IC_{50} = 2.16 ± 0.09 μM) and rivastigmine (IC_{50} = 4.63 ± 0.1 μM) implying the signifance of three methoxy groups in 3,4,5-position. From structure-activity point of view, the inhibitory potency of the synthesized mono-substituted derivatives bearing different substituents was found to be in the order: -OH group > -OMe group > -Cl group > -Me group > -CF_3 group > -CN group implying that electron-donating groups afforded good to moderate inhibitory activity. Di-substitution on the ring with groups such as Methoxy or Methyl; inhibitory activity was found to decrease in case of Methyl group. Selectivity index of the synthesized derivatives was observed to be in the range between 1.60 and 21.59.

In the term of BuChE inhibitory activity, compound **5o** (IC_{50} = 1.17 ± 0.06 μM) showed enhanced inhibitory activity than the standard drugs galantamine (IC_{50} = 1.41 ± 0.12 μM) and rivastigmine (IC_{50} = 4.34 ± 0.14 μM). In addition, compounds **5b** (IC_{50} = 3.462 ± 0.09 μM) and **5j** (IC_{50} = 3.32 ± 0.17 μM) showed better inhibitory activity than standard drug rivastigmine.

2.2.2. Kinetic analysis of AChE and BuChE inhibition

The mechanism for AChE and BuChE inhibitions were elucidated by applying the Lineweaver-Burk plot analysis for the most potent derivative (**5o**). Acetylthiocholine iodide and S-Butyrylthiocholine iodide were used as substrate for AChE and BuChE inhibitions respectively. Lineweaver-Burk plot of 1/V versus substrate 1/[S] in the presence of different inhibitor concentrations (5, 10 and 20 μM) resulted into a series of straight lines as shown in Fig. 2**a and b** for AChE and BuChE respectively. In both AChE and BuChE, slopes and intercepts are increasing with increasing concentration of inhibitor **5o** ascribing a mixed-type inhibition. A secondary plot of slope versus concentration of inhibitor was plotted and the inhibition constant (K_i) was calculated which was found to be 2.354 μM and 7.054 μM (Fig. 2**c and 2d** respectively).

2.2.3. Antioxidant activity assay

The antioxidant activity of compounds **5(a-o)** was performed against DPPH and hydrogen peroxide scavenging.

2.2.3.1. DPPH radical scavenging assay.

Radical scavenging activity by DPPH is a popular and rapid assay used to access the antioxidant activity. Compounds of different concentrations were subjected for scavenging activity using stable DPPH radical and the decrease in absorbance was monitored by visible spectrophotometer at 517 nm. The results are summarized in Table 1. The IC_{50} values of tested compounds ranged between 30.26 and 49.29 μM implying that the test compounds possessed some scavenging activity. Compounds **5o** was the most potent compounds with IC_{50} value 30.26 ± 0.13 μM when compared to the ascorbic acid (IC_{50} = 27.18 ± 0.1 μM).

2.2.3.2. Hydrogen peroxide scavenging assay.

Hydrogen peroxide (H_2O_2) is an oxidizing agent resulting from aerobic metabolisms. It generates hydroxyl radical through Fenton reaction [35]. These hydroxyl cause severe tissues damages by disrupting cell membranes or altering the proteins/ DNA's structure resulting in oxidative stress [36]. Hence it is necessary to scavenge H_2O_2 in the cells to avoid cellular cytotoxicity. The IC_{50} values of tested compounds examined ranged from 28.07 to 48.84 μM indicating that the test compounds acquire certain scavenging activity. The results are represented in Table 1. Compounds **5o** was the most potent with IC_{50} value 28.07 ± 0.17 μM when compared to ascorbic acid (IC_{50} = 23.94 ± 0.11 μM) while other test compounds exhibited notable scavenging activity.

2.2.4. Determination of cell viability

In order to determine the therapeutic potential of synthesized compounds, cell viability assay was conducted in N2a neuroblastoma cell by using MTT assay. For this purpose, cells were exposed to the test compounds at higher concentration (20 and 40 μM) for 24 h and cell viability was determined. The results are outlined in Table 2. The results indicated that none of the test compounds demonstrated toxicity to the neuron cells at any tested concentrations. The screening results of the compounds were also compared to standard drugs indicating no cytotoxicity in N2a cells as shown in Fig. 3.

2.2.5. Neuroprotective studies against H_2O_2-induced stress

It is hypothesized that oxidative stress plays an important role in the progression of AD contributing to several degenerative diseases related

Table 1
Inhibitory Cholinesterase activity and antioxidant scavenging activity of compounds **5(a-o)**.

Code	Cholinesterase activity (IC_{50} ± SD)[a]		SI for AChE[b]	Antioxidant activity (IC_{50} ± SD) [a]	
	AChE	BuChE		DPPH	H_2O_2
5a	8.79 ± 0.16	30.17 ± 0.19	3.43	44.97 ± 0.25	44.84 ± 0.18
5b	3.44 ± 0.14	10.37 ± 0.12	3.01	47.44 ± 0.14	43.83 ± 0.15
5c	0.67 ± 0.12	3.46 ± 0.09	5.16	46.67 ± 0.17	41.51 ± 0.11
5d	0.95 ± 0.21	4.54 ± 0.17	4.75	38.28 ± 0.19	42.91 ± 0.17
5e	5.03 ± 0.23	8.06 ± 0.26	1.60	41.49 ± 0.21	42.21 ± 0.24
5f	3.64 ± 0.19	17.54 ± 0.22	4.85	37.54 ± 0.27	33.58 ± 0.19
5g	0.96 ± 0.26	16.91 ± 0.15	17.61	37.43 ± 0.14	30.48 ± 0.22
5h	0.54 ± 0.11	5.73 ± 0.21	10.61	49.29 ± 0.19	46.56 ± 0.18
5i	0.92 ± 0.14	19.87 ± 0.18	21.59	43.44 ± 0.24	44.61 ± 0.19
5j	0.57 ± 0.17	3.32 ± 0.17	5.82	36.59 ± 0.17	43.36 ± 0.24
5k	5.12 ± 0.19	17.34 ± 0.16	3.38	45.58 ± 0.25	44.79 ± 0.27
5l	5.26 ± 0.19	11.72 ± 0.13	2.22	45.82 ± 0.29	48.84 ± 0.26
5m	7.35 ± 0.09	12.64 ± 0.12	1.71	37.93 ± 0.14	42.14 ± 0.24
5n	0.74 ± 0.17	6.28 ± 0.11	8.48	37.54 ± 0.18	33.58 ± 0.14
5o	0.41 ± 0.16	1.17 ± 0.13	2.84	30.26 ± 0.13	28.07 ± 0.17
Rivastigmine	4.63 ± 0.12	4.34 ± 0.14	0.93	–	–
Galantamine	2.16 ± 0.09	1.41 ± 0.12	0.65	–	–
Ascorbic acid	–	–	–	27.18 ± 0.1	23.94 ± 0.11

[a] IC_{50} values = mean (n ± SD). (Concentration that inhibits 50% in μM, and the data were obtained from triplicate runs).
[b] Selectivity Index = IC_{50} (BuChE)/IC_{50} (AChE).

to aging such as cancer, epilepsy and AD [37]. Therefore, we investigated neuroprotective effect of test compounds for H_2O_2-induced stress in N2a cells. For this, N2a cells were pretreated with test compounds (20 and 40 μM) for 2 h and then exposed to 100 μM H_2O_2 for 24 h. The results are summarized in Table 2 which reveals that the tested derivatives exhibited significant neuroprotective effect. N2a cells exposed to 100 μM H_2O_2 for 24 h were taken as negative control. The compounds were also compared with the reference drugs and it was found that they showed comparable results (Fig. 4).

2.2.6. DNA damage protection assay

Aforementioned, H_2O_2 is proposed to be leading cause of oxidative stress resulting in AD progression, we examined DNA damage protection assay using different concentrations of compound **5o** (10, 20 and 40 μM). For this purpose, Agarose gel electrophoresis was performed where supercoiled pBR322 plasmid DNA was used as a substrate and Fenton's reagent was used as DNA damaging agent. During the electrophoresis, DNA damage was visualised by the shearing or disappearance of the band. From Fig. 5, it is evident that compound **5o** displayed maximal DNA damage protection at 20 and 40 μM (Fig. 5; Lane 4 and 5 respectively) in comparison with plasmid DNA incubated with Fenton's reagent (Fig. 5; Lane 2).

2.3. Molecular docking

To understand the binding mode, the most active compound **5o** was docked with AChE. The docking analysis revealed that compound **5o** interacts with both the CAS and the PAS of AChE (Fig. 6). Compound **5o** possessed three H-bonding interactions: One at the PAS with Asp72, one at acyl binding pocket with Phe288 and the other CAS with Ser200 residue. Compound **5o** showed two π-π interactions with Trp279 and Tyr334 residues at the PAS while one π-π interaction at anionic subsite with Phe330 residue. When rivastigmine and galantamine were docked into the active site of AChE, similar interactions were observed as observed with compound **5o**. The orientation of compound **5o**, rivastigmine and galantamine with AChE is represented in Fig. 6. Also, compound **5o** displayed high binding affinity than standards (Table 3). Based on these assessments, it can be stated that compound **5o** has ability as that of standard drug to bind in the active site of the protein. The results also corroborate with the kinetic studies i.e. compound **5o** exhibit mixed type inhibition.

Crystal structure of human BuChE was used in the docking studies since the crystal structure of BuChE from equine serum is not reported. Fig. 7 displays 3D and 2D docking poses of compound **5o**, rivastigmine and galantamine. Compound **5o** displayed two Hydrogen-bonding interactions with Glu197 residue at the PAS while Ser287 residue in the acyl pocket. Compound **5o** also exhibited π-π stacking interactions with Trp82 of PAS, His438 of CAS and Phe329 of anionic subsite. This explains mixed type inhibition of compound **5o** with BuChE. From Table 3, it is noticeable that compound **5o** displayed high binding affinity than the standard. Also, compound **5o** fits exactly in the binding pocket of BuChE as seen in the standard drugs with similar interaction.

2.4. ADME studies

The synthesized derivatives were analysed for drug-likeness by evaluating with QikProp module of Schrodinger. The pharmacokinetic parameters along with their acceptable range are displayed in Table 4.

2.5. PAINS

PAINS (**P**an-**A**ssay **IN**terference compound**S**) filters are used to clean chemical libraries from substances that are most likely toxic, reactive or unstable and vulnerable to interference with biological testing [38]. Any of the synthesized compounds did not exhibit any PAINS alerts (Table 4).

3. Conclusion

In conclusion, we designed, synthesized and characterised 15 novel dihydropyranoindole derivatives containing sulphonamide group and evaluated for *in-vitro* anti-cholinesterase activity. The result revealed that all the compounds exhibited potent AChE activity (IC_{50} = 0.41–8.79 μM) when compared to BuChE (IC_{50} = 1.17–30.17 μM). Compound **5o** was most active inhibitor towards both AChE (IC_{50} = 0.41 μM) and BuChE (IC_{50} = 1.17 μM) when compared to standard drugs. Enzyme kinetics and molecular docking studies suggested that compound **5o** shows mixed type inhibition and binds to PAS and CAS of both enzymes. Also, cell viability studies were also performed against N2a cells which suggested that compounds do not impart any cytotoxicity. Further, neuroprotection assay against H_2O_2 were performed in N2a cell line and the compounds were found to be protective in nature. In addition, antioxidant studies using DPPH radical and H_2O_2 were also performed and the results indicated that test compounds possess some antioxidant activity. DNA damage protection assay for compound **5o** suggested that it is protective in nature. ADME studies were also performed which demonstrated good pharmacokinetics.

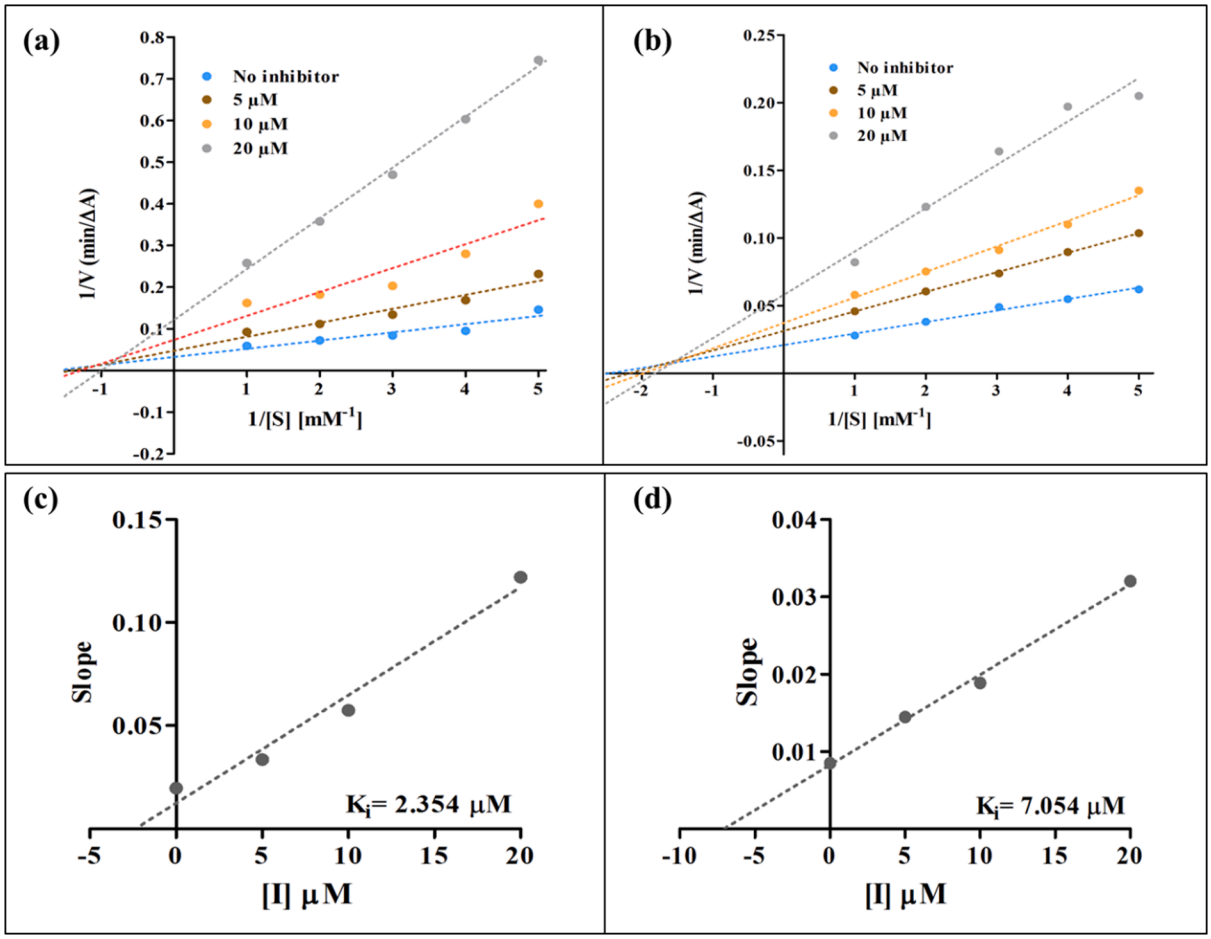

Fig. 2. (**a**) Lineweaver-Burk plot for the inhibition of AChE by compound **5o**, (**b**) Lineweaver-Burk plot for the inhibition of BuChE by compound **5o**, (**c**) Secondary plot for steady-state inhibition constant (Ki) of AChE by compounds **5o** and (**d**) Secondary plot for steady-state inhibition constant (Ki) of BuChE by compounds **5o.**

Table 2
Cell viability and neuroprotection activity of compounds **5(a-o)** against N2a cell line.

Code	Cell viability (%)[a]		Neuroprotection (%)[a]	
	20 µM	40 µM	20 µM	40 µM
5a	88.89 ± 0.95	91.28 ± 2.01	22.45 ± 1.68	39.65 ± 1.19
5b	90.08 ± 1.65	92.67 ± 0.86	27.03 ± 2.15	51.61 ± 0.96
5c	92.48 ± 0.43	90.46 ± 0.81	27.24 ± 2.19	39.53 ± 0.48
5d	89.60 ± 1.02	91.91 ± 1.17	29.56 ± 1.32	50.86 ± 0.90
5e	92.48 ± 1.46	89.46 ± 1.91	27.25 ± 4.80	51.48 ± 0.69
5f	90.08 ± 1.46	89.61 ± 1.44	31.61 ± 1.30	39.53 ± 0.55
5g	90.70 ± 0.51	91.04 ± 1.22	25.79 ± 2.26	41.15 ± 1.59
5h	91.71 ± 0.93	90.46 ± 1.89	28.70 ± 1.62	39.12 ± 0.81
5i	91.76 ± 0.81	89.65 ± 1.97	27.35 ± 3.68	38.75 ± 0.49
5j	91.81 ± 2.02	88.84 ± 0.50	26.65 ± 4.19	39.47 ± 0.78
5k	89.94 ± 1.37	92.52 ± 1.52	28.54 ± 3.52	50.61 ± 0.68
5l	91.04 ± 1.63	92.24 ± 1.01	29.88 ± 3.72	51.02 ± 0.70
5m	90.08 ± 1.31	92.28 ± 0.59	37.53 ± 2.26	50.43 ± 0.43
5n	91.52 ± 2.44	90.97 ± 1.96	39.31 ± 3.52	38.45 ± 0.52
5o	93.34 ± 0.36	92.14 ± 1.20	39.14 ± 2.15	52.26 ± 0.34
Rivastigmine	92.24 ± 1.74	92.72 ± 1.02	40.28 ± 1.21	51.66 ± 1.52
Galantamine	93.19 ± 1.79	92.81 ± 2.90	39.90 ± 1.29	51.75 ± 0.26

[a] Data are expressed as Mean ± SD (three independent experiments).

4. Experimental

4.1. Materials and methods

Acetylcholinesterase from Electrophorus electricus (electric eel) Type VI-S, Butyrylcholinesterase from equine serum lyophilized powder and supercoiled pBR322 plasmid DNA were procured from Sigma Aldrich (India). All the chemicals were purchased from Sigma Aldrich (India) and were used without further purification. Neuro2a cells (N2a) was purchased from National Centre for Cell Sciences (NCCS), Pune, India. MTT, Minimum Essential Medium Eagle (MEM) and antibiotics were purchased from Hi-Media Laboratories Ltd. (Mumbai, India). Fetal bovine serum (FBS), Phosphate buffered saline (PBS) and Trypsin-EDTA was obtained from Thermo scientific (Gibco). The activity was determined by measuring the absorbance on Thermo Scientific Multiskan GO Microplate Spectrophotometer. All the reactions were monitored by using thin layer chromatography (TLC) using Merck silica gel 60 F254 plates. Melting points were measured in open capillary tubes and are uncorrected. FTIR was recorded on Perkin Elmer, Frontier equipment with ATR. ^{1}H NMR (300 MHz) and ^{13}C NMR (75 MHz) were recorded on Bruker AVANCE II using TMS as internal standard in DMSO-d_6. ESI mass spectra were recorded on AB SCIEX 3200 QTRAP mass spectrometer. Elemental analysis was performed on model EA300, Euro Vector, Italy.

4.2. Chemistry

4.2.1. *Synthesis of 1-tosyl-1H-indol-4-ol (2)* [33]

^{t}BuOK (1 mmol) was added to a stirring solution of 4-Hydroxyindole (**1**) (1 mmol) in dry DMF (20 mL), followed by dropwise addition of Tosyl chloride (1 mmol) at 0 °C. The reaction mixture was stirred for 45 min and progress of the reaction was monitored by TLC. After completion, the mixture was poured into water and extracted with ethyl acetate. The filtrate was concentrated under reduced pressure and mixture

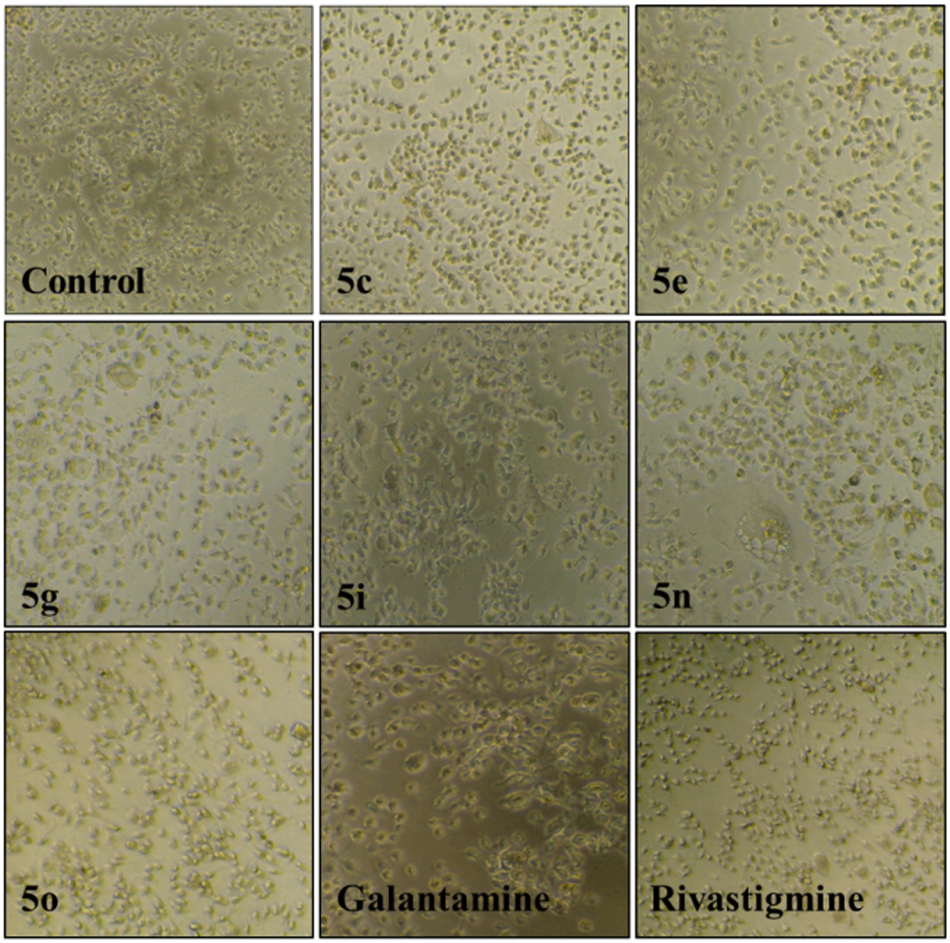

Fig. 3. Microscopic photographs of N2a cells treated with compound **5c, 5e, 5g, 5i, 5n, 5o, galantamine** and **rivastigmine** (40 μM). Data are expressed as mean ± SD in triplicates.

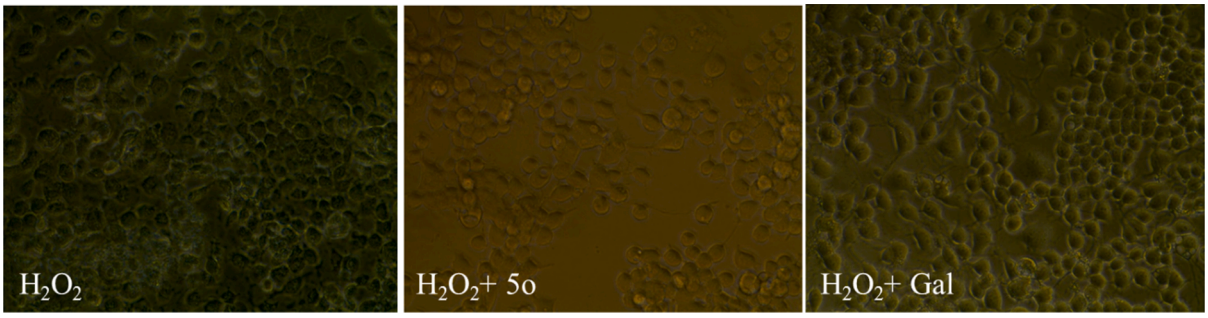

Fig. 4. Microscopic photographs of N2a cells treated with H_2O_2; H_2O_2 + Compound **5o** and H_2O_2 + Galantamine (40 μM). Data are expressed as mean ± SD in triplicates.

was purified by column chromatography with 20% ethyl acetate in *n*-hexane afford titled compound.

4.2.1.1. 1-tosyl-1H-indol-4-ol (2). Buff solid, Yield = 80%; M.P: 143–145 °C. **IR (υ_{max}/cm^{-1}):** 3454 (OH), 1593 (C=C), 1160 (SO_2). **^{1}H NMR (300 MHz, $CDCl_3$)** δ = 77.75 (d, *J* = 8.0 Hz, 2H, Ar-H), 7.57 (d, *J* = 8.5 Hz, 1H, Ar-H), 7.48 (d, *J* = 3.6 Hz, 1H, Ar-H), 7.21 (d, *J* = 7.9 Hz, 2H, Ar-H), 7.14 (t, *J* = 8.1 Hz, 1H, Ar-H), 6.74 (d, *J* = 3.6 Hz, 1H, Ar-H), 6.61 (d, *J* = 7.7 Hz, 1H, Ar-H), 5.28 (s, 1H, OH), 2.33 (s, 3H, CH_3). **^{13}C NMR (75 MHz, $CDCl_3$)** δ = 149.15, 145.12, 136.77, 135.40, 130.08, 127.06, 125.35, 120.20, 108.48, 106.80, 105.527, 21.75 (CH_3). **MS (ESI)** ***m/z***: 288.2 $(M+1)^+$. **Elemental analysis for $C_{15}H_{13}NO_3S$:** C, 62.70; H, 4.56; N, 4.87; found: C, 62.64; H, 4.42; N, 4.61.

4.2.2. Synthesis of dihydropyranoindole 5(a-o)

Triethylamine (1 mmol) was added to a mixture of 1-tosyl-1H-indol-4-ol (**2**) (1 mmol), substituted aldehyde **3 (a-o)** (1 mmol) and malononitrile (**4**) (1 mmol) in 10 mL ethanol. The reaction was refluxed at 80 °C and the solid formed was cooled and filtered. The residue obtained was recrystallized using ethanol to afford pure solid in good to excellent yield.

4.2.2.1. Ethyl 2-amino-3-cyano-7-tosyl-4,7-dihydropyrano[2,3-e]indole-4-carboxylate (5a). White solid, Yield: 94%, M.P: 197–199 °C. **IR (υ_{max}/**

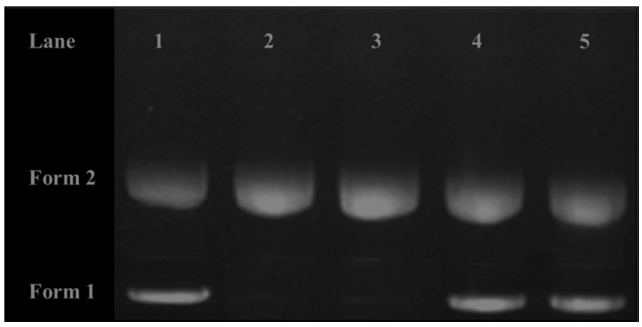

Fig. 5. Lane 1-pBR322 (control), Lane 2-pBR322 + Fenton's reagent, Lane 3-pBR322 + Fenton's reagent + **5o** (10 μM), Lane 4-pBR322 + Fenton's reagent + **5o** (20 μM), Lane 5-pBR322 + Fenton's reagent + **5o** (40 μM).

cm^{-1}): 3324 (NH_2), 2203 (CN), 1165, 1181 (SO_2). **^{1}H NMR (300 MHz, DMSO)** δ = 7.87 (t, *J* = 5.7 Hz, 3H, Ar-H), 7.72 (d, *J* = 8.5 Hz, 1H, Ar-H), 7.38 (d, *J* = 8.1 Hz, 2H, Ar-H), 7.28–7.19 (m, 3H, NH_2, Ar-H), 6.75 (d, *J* = 3.6 Hz, 1H, Ar-H), 4.52 (s, 1H, CH), 4.08 (q, *J* = 7.1 Hz, 2H, CH_2), 2.31 (s, 3H, CH_3), 1.14 (t, *J* = 7.1 Hz, 3H, CH_3). **^{13}C NMR (75 MHz, DMSO)** δ = 171.82, 161.09, 145.84, 141.57, 134.60, 133.82, 130.32, 127.60, 126.77, 124.83, 119.75, 119.09, 111.74, 109.52 (CN), 104.56, 61.10 (CH), 50.67 (CH_2), 20.98 (CH_3), 13.96 (CH_3). **MS (ESI)** ***m/z***: 438.4 $(M+1)^+$. **Elemental analysis for $C_{22}H_{19}N_3O_5S$:** C, 60.40; H, 4.38; N, 9.61; found: C, 60.24; H, 4.20; N, 9.42.

4.2.2.2. 2-amino-4-(2-methoxyphenyl)-7-tosyl-4,7-dihydropyrano[2,3-e] indole-3-carbonitrile (5b). White solid, Yield: 94%, M.P: 266–268 °C. **IR (υ_{max}/cm^{-1}):** 3319 (NH_2), 2197 (CN), 1185 (SO_2). **^{1}H NMR (300 MHz, DMSO)** δ = 7.83 (t, *J* = 6.4 Hz, 3H, Ar-H), 7.58 (d, *J* = 8.6 Hz, 1H, Ar-H), 7.34 (d, *J* = 8.1 Hz, 2H, Ar-H), 7.17 (t, *J* = 7.2 Hz, 1H, Ar-H), 7.09–6.93 (m, 5H, NH_2, Ar-H), 6.88–6.74 (m, 2H, Ar-H), 5.15 (s, 1H, CH), 3.76 (s, 3H, OCH_3), 2.27 (s, 3H, CH_3). **^{13}C NMR (75 MHz, DMSO)** δ = 160.59, 156.23, 145.71, 141.13, 133.89, 133.80, 133.57, 130.27, 128.75, 128.12, 127.18, 126.72, 124.99, 120.81, 120.46, 118.86, 117.28, 111.64, 109.41 (CN), 104.74, 55.67 (CH), 55.43 (OCH_3), 20.96 (CH_3). **MS (ESI)** ***m/z***: 472.3 $(M+1)^+$. **Elemental analysis for $C_{26}H_{21}N_3O_4S$:** C, 66.23; H, 4.49; N, 8.91; found: C, 66.07; H, 4.27; N, 8.23.

4.2.2.3. 2-amino-4-(3-methoxyphenyl)-7-tosyl-4,7-dihydropyrano[2,3-e] indole-3-carbonitrile (5c). White solid, Yield: 95%, M.P: 222–224 °C. **IR (υ_{max}/cm^{-1}):** 3301 (NH_2), 2198 (CN), 1181 (SO_2). **^{1}H NMR (300 MHz, DMSO)** δ = 7.84 (dd, *J* = 5.9, 3.8 Hz, 3H, Ar-H), 7.62 (d, *J* = 8.6 Hz, 1H, Ar-H), 7.35 (d, *J* = 8.2 Hz, 2H, Ar-H), 7.19 (dd, *J* = 8.8, 7.6 Hz, 1H, Ar-H), 7.07–6.98 (m, 3H, NH_2, Ar-H), 6.80–6.72 (m, 4H, Ar-H), 4.78 (s, 1H, CH), 3.69 (s, 3H, OCH_3), 2.28 (s, 3H, CH_3). **^{13}C NMR (75 MHz, DMSO)** δ = 160.01, 159.33, 147.45, 145.76, 140.78, 133.89, 130.30, 129.81, 127.32, 126.74, 125.53, 120.34, 119.68, 118.93, 116.98, 113.59, 111.64, 109.51 (CN), 104.70, 56.21 (CH), 54.91 (OCH_3), 20.96 (CH_3). **MS (ESI)** ***m/z***: 472.0 $(M+1)^+$. **Elemental analysis for $C_{26}H_{21}N_3O_4S$:** C, 66.23; H, 4.49; N, 8.91; found: C, 66.19; H, 4.21; N, 8.64.

4.2.2.4. 2-amino-4-(4-methoxyphenyl)-7-tosyl-4,7-dihydropyrano[2,3-e] indole-3-carbonitrile (5d). White solid, Yield: 94%, M.P: 221–223 °C. **IR (υ_{max}/cm^{-1}):** 3324 (NH_2), 2200 (CN), 1173 (SO_2). **^{1}H NMR (300 MHz, DMSO)** δ = 7.84 (t, *J* = 6.3 Hz, 3H, Ar-H), 7.60 (d, *J* = 8.6 Hz, 1H, Ar-H), 7.37 (d, *J* = 8.1 Hz, 2H, Ar-H), 7.10 (d, *J* = 8.5 Hz, 2H, Ar-H), 7.04–6.90 (m, 3H, NH_2, Ar-H), 6.84 (d, *J* = 8.5 Hz, 2H, Ar-H), 6.76 (d, *J* = 3.5 Hz, 1H, Ar-H), 4.74 (s, 1H, CH), 3.70 (s, 3H, CH_3), 2.30 (s, 3H, CH_3). **^{13}C NMR (75 MHz, DMSO)** δ = 159.76, 158.04, 145.77, 140.71, 138.04, 133.90, 133.78, 130.32, 128.53, 127.26, 126.75, 125.61, 120.39, 118.90, 117.41, 113.98, 109.46 (CN), 104.70, 56.67 (CH), 54.97 (OCH_3), 20.99 (CH_3). **MS (ESI)** ***m/z***: 472.3 $(M+1)^+$. **Elemental analysis for $C_{26}H_{21}N_3O_4S$:** C, 66.23; H, 4.49; N, 8.91; found: C, 66.10; H, 4.22; N, 8.54.

4.2.2.5. 2-amino-4-(p-tolyl)-7-tosyl-4,7-dihydropyrano[2,3-e]indole-3-carbonitrile (5e). White solid, Yield: 94%, M.P: 267–269 °C. **IR (υ_{max}/cm^{-1}):** 3302 (NH_2), 2200 (CN), 1190 (SO_2). **^{1}H NMR (300 MHz, DMSO)** δ = 7.84 (t, *J* = 5.6 Hz, 3H, Ar-H), 7.61 (d, *J* = 8.6 Hz, 1H, Ar-H), 7.36 (d, *J* = 8.2 Hz, 2H, Ar-H), 7.07 (s, 4H, Ar-H), 7.00 (s, 2H, NH_2), 6.93 (d, *J* = 8.6 Hz, 1H, Ar-H), 6.75 (d, *J* = 3.6 Hz, 1H, Ar-H), 4.75 (s, 1H, CH), 2.30 (s, 3H, CH_3), 2.23 (s, 3H, CH_3). **^{13}C NMR (75 MHz, DMSO)** δ = 159.83, 145.76, 142.99, 140.75, 135.89, 133.90, 133.81, 130.32, 129.19, 127.39, 127.29, 126.75, 125.60, 120.36, 118.90, 117.25, 109.47 (CN), 104.66, 56.48 (CH), 20.98 (CH_3), 20.54 (CH_3). **MS (ESI)** ***m/z***: 456 $(M+1)^+$. **Elemental analysis for $C_{26}H_{21}N_3O_3S$:** C, 68.55; H, 4.65; N, 9.22; found: C, 68.31; H, 4.23; N, 9.17.

4.2.2.6. 2-amino-4-(3-chlorophenyl)-7-tosyl-4,7-dihydropyrano[2,3-e] indole-3-carbonitrile (5f). White solid, Yield: 94%, M.P: 247–249 °C. **IR (υ_{max}/cm^{-1}):** 3322 (NH_2), 2199 (CN), 1170 (SO_2). **^{1}H NMR (300 MHz, DMSO)** δ = 7.98–7.78 (m, 3H, Ar-H), 7.64 (d, *J* = 8.6 Hz, 1H, Ar-H), 7.45–7.21 (m, 5H, Ar-H), 7.22–7.07 (m, 3H, Ar-H), 6.98 (d, *J* = 8.7 Hz, 1H, Ar-H), 6.77 (d, *J* = 3.5 Hz, 1H, Ar-H), 4.88 (s, 1H, CH), 2.29 (s, 3H, CH_3). **^{13}C NMR (75 MHz, DMSO)** δ = 160.07, 148.33, 145.79, 140.85, 134.02, 133.89, 133.19, 130.67, 130.31, 127.43, 127.23, 126.88, 126.76, 126.32, 125.47, 120.17, 118.98, 116.34, 109.69 (CN), 104.68, 55.75 (CH), 20.97 (CH_3). **MS (ESI)** ***m/z***: 476.3 $(M+1)^+$. **Elemental analysis for $C_{25}H_{18}ClN_3O_3S$:** C, 63.09; H, 3.81; N, 8.83; found: C, 62.98; H, 3.51; N, 8.64.

4.2.2.7. 2-amino-4-(4-chlorophenyl)-7-tosyl-4,7-dihydropyrano[2,3-e] indole-3-carbonitrile (5 g). White solid, Yield: 94%, M.P: 283–285 °C. **IR (υ_{max}/cm^{-1}):** 3321 (NH_2), 2199 (CN), 1173 (SO_2). **^{1}H NMR (300 MHz, DMSO)** δ = 7.96–7.79 (m, 3H, Ar-H), 7.63 (d, *J* = 8.6 Hz, 1H, Ar-H), 7.48–7.31 (m, 4H, Ar-H), 7.22 (d, *J* = 8.4 Hz, 2H, Ar-H), 7.08 (s, 2H, NH_2), 6.94 (d, *J* = 8.6 Hz, 1H, Ar-H), 6.76 (d, *J* = 3.6 Hz, 1H, Ar-H), 4.86 (s, 1H, CH), 2.31 (s, 3H, CH_3).

^{13}C NMR (75 MHz, DMSO) δ = 159.93, 145.81, 144.86, 140.82, 133.94, 133.88, 131.41, 130.34, 129.40, 128.64, 127.39, 126.77, 125.50, 120.20, 118.95, 116.56, 109.62 (CN), 104.66, 55.95 (CH), 20.99 (CH_3). **MS (ESI)** ***m/z***: 475 $(M)^{+\cdot}$ **Elemental analysis for $C_{25}H_{18}ClN_3O_3S$:** C, 63.09; H, 3.81; N, 8.83; found: C, 63.00; H, 3.04; N, 8.43.

4.2.2.8. 2-amino-4-(3-fluorophenyl)-7-tosyl-4,7-dihydropyrano[2,3-e] indole-3-carbonitrile (5 h). White solid, Yield: 95%, M.P: 284–286 °C. **IR (υ_{max}/cm^{-1}):** 3321 (NH_2), 2205 (CN), 1178 (SO_2). **^{1}H NMR (300 MHz, DMSO)** δ = 7.98–7.79 (m, 3H, Ar-H), 7.64 (d, *J* = 8.6 Hz, 1H, Ar-H), 7.34 (dd, *J* = 11.3, 4.9 Hz, 3H, Ar-H), 7.11 (s, 2H, NH_2), 7.07–6.93 (m, 4H, Ar-H), 6.77 (d, *J* = 3.6 Hz, 1H, Ar-H), 4.88 (s, 1H, CH), 2.29 (s, 3H, CH_3). **^{13}C NMR (75 MHz, DMSO)** δ = 162.20 (d, $^1J_{FC}$ = 244.4 Hz), 160.08, 148.73, 148.64, 145.82, 140.82, 133.91 (d, $^3J_{FC}$ = 11.0 Hz), 130.70 (d, $^3J_{FC}$ = 8.2 Hz), 130.30, 127.36, 126.74, 125.44, 123.55, 120.22, 119.00, 116.40, 114.14 (d, $^2J_{FC}$ = 21.5 Hz), 113.68 (d, $^2J_{FC}$ = 21.2 Hz), 109.62 (CN), 104.81, 55.80 (CH), 20.95 (CH_3). **MS (ESI)** ***m/z***: 460.3 $(M+1)^+$. **Elemental analysis for $C_{25}H_{18}FN_3O_3S$:** C, 65.35; H, 3.95; N, 9.14; found: C, 65.20; H, 3.74; N, 9.09.

4.2.2.9. 2-amino-4-(4-fluorophenyl)-7-tosyl-4,7-dihydropyrano[2,3-e] indole-3-carbonitrile (5i). White solid, Yield: 93%, M.P: 280–282 °C. **IR (υ_{max}/cm^{-1}):** 3324 (NH_2), 2200 (CN), 1176 (SO_2). **^{1}H NMR (300 MHz, DMSO)** δ = 7.85 (dd, *J* = 5.6, 4.8 Hz, 3H, Ar-H), 7.62 (d, *J* = 8.6 Hz, 1H, Ar-H), 7.37 (d, *J* = 8.2 Hz, 2H, Ar-H), 7.23 (dd, *J* = 8.5, 5.6 Hz, 2H, Ar-H), 7.12 (d, *J* = 8.8 Hz, 2H, Ar-H), 7.07 (d, *J* = 7.8 Hz, 2H, NH_2), 6.94 (d, *J* = 8.6 Hz, 1H, Ar-H), 6.77 (d, *J* = 3.6 Hz, 1H, Ar-H), 4.85 (s, 1H, CH), 2.30 (s, 3H, CH_3). **^{13}C NMR (75 MHz, DMSO)** δ = 160.99 (d, $^1J_{FC}$ = 246.7 Hz), 159.88, 145.79, 142.11 (d, $^3J_{FC}$ = 3.0 Hz), 140.80, 133.89,

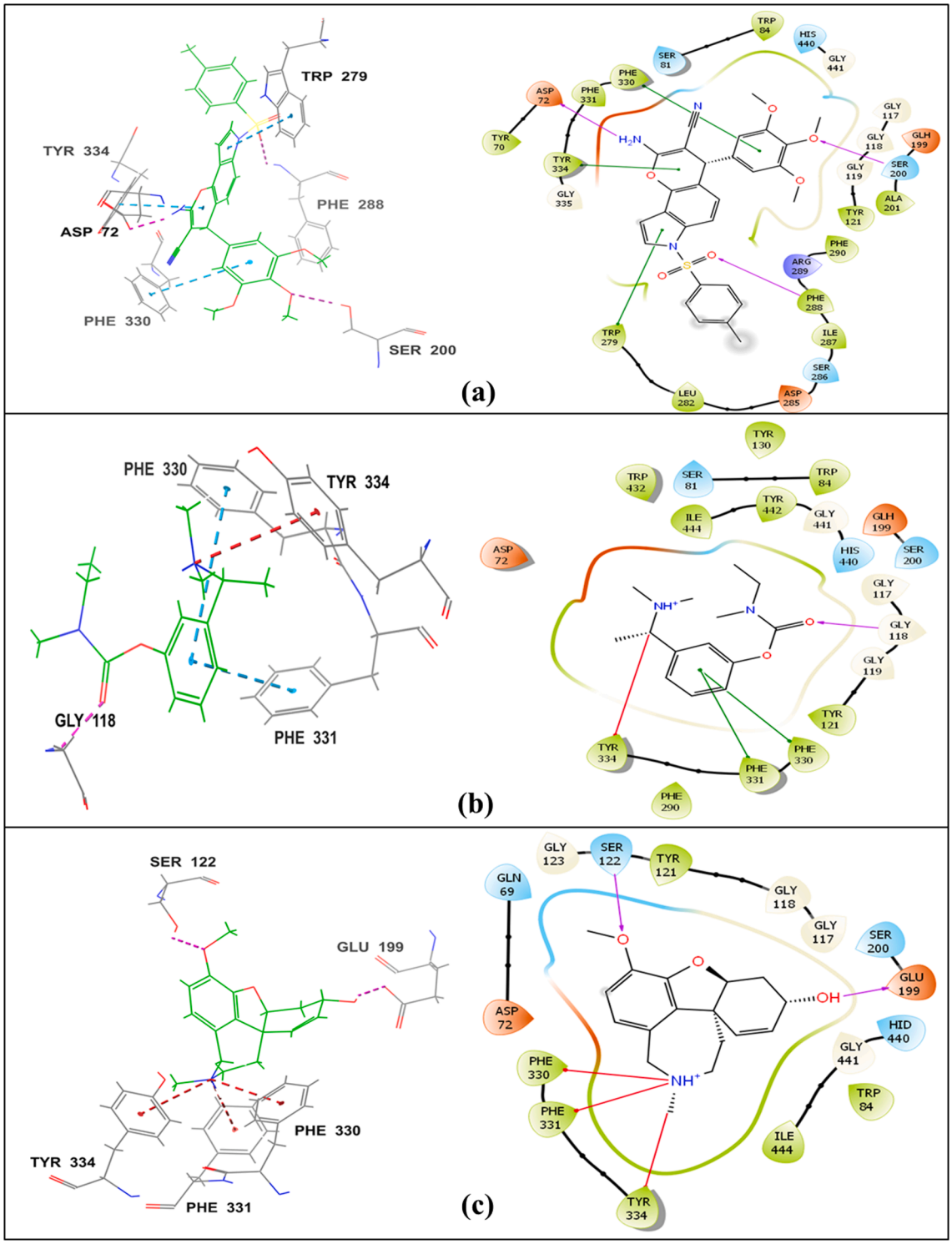

Fig. 6. 3D and 2D docking pose of (**a**) compound **5o**, (**b**) rivastigmine and (**c**) galantamine in the active site of AChE.

130.32, 129.39 (d, $^{3}J_{FC}$ = 8.2 Hz), 127.36, 126.76, 125.52, 120.26, 118.95, 116.88, 115.38 (d, $^{2}J_{FC}$ = 21.2 Hz), 109.58 (CN), 104.69, 56.28 (CH), 20.98 (CH_3). **MS (ESI) *m/z***: 459.3 $(M)^+$. **Elemental analysis for $C_{25}H_{18}FN_3O_3S$:** C, 65.35; H, 3.95; N, 9.14; found: C, 65.14; H, 3.75; N, 9.02.

4.2.2.10. 2-amino-4-(3-hydroxyphenyl)-7-tosyl-4,7-dihydropyrano[2,3-e] indole-3-carbonitrile (5j). White solid, Yield: 94%, M.P: 275–278 °C. **IR (υ_{max}/cm^{-1})**: 3600 (OH), 3321 (NH_2), 2202 (CN), 1179 (SO_2). **^{1}H NMR (300 MHz, DMSO)** δ = 9.34 (s, 1H, OH), 7.85 (t, J = 5.4 Hz, 3H, Ar-H), 7.63 (d, J = 8.6 Hz, 1H, Ar-H), 7.35 (d, J = 8.2 Hz, 2H, Ar-H), 7.18–6.92 (m, 4H, NH_2, Ar-H), 6.78 (d, J = 3.6 Hz, 1H, Ar-H), 6.71–6.52 (m, 3H, Ar-H), 4.70 (s, 1H, CH), 2.27 (s, 3H, CH_3). **^{13}C NMR (75 MHz, DMSO)** δ = 159.96, 157.40, 147.32, 145.80, 140.74, 133.81, 133.75, 130.26, 129.65, 127.20, 126.68, 125.49, 120.44, 118.95, 118.17, 117.09, 114.14, 113.91, 109.49 (CN), 104.87, 56.45 (CH), 20.90 (CH_3). **MS (ESI) *m/z***: 456.1 (M−1).

Elemental analysis for $C_{25}H_{19}N_3O_4S$: C, 65.63; H, 4.19; N, 9.18;

Table 3
Comparative interaction analysis of compound **5o** with standard AChE/BuChE inhibitors.

Enzyme	Compound	Glide score	Glide energy (kJ/mol)	Interacting residues
AChE	**5o**	−8.138	−62.436	**Hydrogen bonding:** Asp72, Ser200, Phe288 **Hydrophobic interactions:** Trp279, Phe330, Tyr334
	Rivastigmine	−9.788	−38.221	**Hydrogen bonding:** Gly118 **Hydrophobic interactions:** Phe330, Phe331, Tyr334
	Galantamine	−12.546	−38.576	**Hydrogen bonding:** Ser122, Glu199 **Hydrophobic interactions:** Phe330, Phe331, Tyr334
BuChE	**5o**	−7.842	−58.929	**Hydrogen bonding:** Glu197, Ser287 **Hydrophobic interactions:** Trp82, Phe329, His438
	Rivastigmine	−6.144	−40.857	**Hydrogen bonding:** Glu197, Asn328 **Hydrophobic interactions:** Phe329
	Galantamine	−6.311	−38.447	**Hydrogen bonding:** Thr120, Glu197 **Hydrophobic interactions:** Trp82, Phe329

found: C, 65.52; H, 4.11; N, 9.12

4.2.2.11. 2-amino-7-tosyl-4-(4-(trifluoromethyl)phenyl)-4,7-dihydropyrano[2,3-e]indole-3-carbonitrile (5 k). White solid, Yield: 95%, M.P: 244–244 °C. **IR (υ_{max}/cm^{-1}):** 3320 (NH_2), 2200 (CN), 1173 (SO_2). **^{1}H NMR (300 MHz, DMSO)** δ = 7.93–7.81 (m, 3H, Ar-H), 7.65 (dd, J = 10.5, 8.6 Hz, 3H, Ar-H), 7.40 (dd, J = 14.5, 7.7 Hz, 4H, Ar-H), 7.14 (s, 2H, NH_2), 6.96 (d, J = 8.6 Hz, 1H, Ar-H), 6.78 (d, J = 3.7 Hz, 1H, Ar-H), 4.97 (s, 1H, CH), 2.30 (s, 3H, CH_3). **^{13}C NMR (75 MHz, DMSO)** δ = 160.03, 150.38, 145.82, 140.92, 134.04, 133.89, 130.33, 128.39, 127.47 (t, J = 15.8 Hz, CF_3), 126.76, 125.97, 125.69, 125.64, 125.59, 125.48, 120.13, 119.00, 116.13, 109.71 (CN), 104.66, 55.65 (CH), 20.98 (CH_3). **MS (ESI) *m/z*:** 510.6 $(M+1)^+$. **Elemental analysis for $C_{26}H_{18}F_3N_3O_3S$:** C, 61.29; H, 3.56; N, 8.25; found: C, 61.10; H, 3.25; N, 8.07.

4.2.2.12. 2-amino-4-(4-cyanophenyl)-7-tosyl-4,7-dihydropyrano[2,3-e]indole-3-carbonitrile (5 l). White solid, Yield: 95%, M.P: 233–235 °C. **IR (υ_{max}/cm^{-1}):** 3320 (NH_2), 2202 (CN), 1180 (SO_2). **^{1}H NMR (300 MHz, DMSO)** δ = 7.85 (d, J = 8.6 Hz, 3H, Ar-H), 7.74 (d, J = 8.1 Hz, 2H, Ar-H), 7.64 (d, J = 8.6 Hz, 1H, Ar-H), 7.36 (dd, J = 19.3, 8.1 Hz, 4H, Ar-H), 7.20 (s, 2H, NH_2), 6.95 (d, J = 8.6 Hz, 1H, Ar-H), 6.78 (d, J = 3.5 Hz, 1H, Ar-H), 4.97 (s, 1H, CH), 2.26 (s, 3H, CH_3). **^{13}C NMR (75 MHz, DMSO)** δ = 160.16, 151.12, 145.79, 140.91, 134.06, 133.78, 132.70, 130.26, 128.53, 127.41, 126.72, 125.37, 120.09, 119.07, 118.62, 115.82, 109.72 (CN), 109.68 (CN), 104.80, 55.36 (CH), 20.91 (CH_3). **MS (ESI) *m/z*:** 469.0 $(M+3)^+$. **Elemental analysis for $C_{26}H_{18}N_4O_3S$:** C, 66.94; H, 3.89; N, 12.01; found: C, 66.65; H, 3.68; N, 11.89.

4.2.2.13. 2-amino-4-(3,5-dimethylphenyl)-7-tosyl-4,7-dihydropyrano[2,3-e]indole-3-carbonitrile (5 m). White solid, Yield: 94%, M.P: 263–265 °C. **IR (υ_{max}/cm^{-1}):** 3328 (NH_2), 2198 (CN), 1187 (SO_2). **^{1}H NMR (300 MHz, DMSO)** δ = 7.87–7.81 (m, 3H, Ar-H), 7.60 (d, J = 8.6 Hz, 1H, Ar-H), 7.33 (d, J = 7.4 Hz, 2H, Ar-H), 7.04–6.93 (m, 3H, NH_2, Ar-H), 6.78 (t, J = 4.8 Hz, 4H, Ar-H), 4.69 (s, 1H, CH), 2.26 (s, 3H, CH_3), 2.17 (s, 6H, 2 × CH_3). **^{13}C NMR (75 MHz, DMSO)** δ = 159.89, 145.86, 145.74, 140.71, 137.60, 133.88, 133.83, 130.28, 128.36, 127.27, 126.74, 125.60, 125.20, 120.42, 118.93, 117.17, 109.49 (CN), 104.73, 56.44 (CH), 20.95 (CH_3), 20.87 (CH_3). **MS (ESI) *m/z*:** 470.6 $(M+1)^+$. **Elemental analysis for $C_{27}H_{23}N_3O_3S$:** C, 69.06; H, 4.94; N, 8.95; found: C, 69.00; H, 4.72; N, 8.80.

4.2.2.14. 2-amino-4-(2,5-dimethoxyphenyl)-7-tosyl-4,7-dihydropyrano[2,3-e]indole-3-carbonitrile (5n). White solid, Yield: 94%, M.P: 199–201 °C. **IR (υ_{max}/cm^{-1}):** 3296 (NH_2), 2202 (CN), 1175 (SO_2). **^{1}H NMR (300 MHz, DMSO)** δ = 7.82 (t, J = 5.5 Hz, 3H, Ar-H), 7.59 (d, J = 8.6 Hz, 1H, Ar-H), 7.32 (d, J = 8.2 Hz, 2H, Ar-H), 7.03–6.95 (m, 3H, NH_2, Ar-H), 6.92 (d, J = 8.9 Hz, 1H, Ar-H), 6.79–6.71 (m, 2H, Ar-H), 6.56 (d, J = 2.9 Hz, 1H, Ar-H), 5.09 (s, 1H, CH), 3.67 (s, 3H, OCH_3), 3.58 (s, 3H, OCH_3), 2.25 (s, 3H, CH_3). **^{13}C NMR (75 MHz, DMSO)** δ = 160.61, 153.28, 150.56, 145.70, 141.07, 134.76, 133.85, 130.24, 127.20, 126.69, 124.97, 120.44, 118.86, 117.04, 115.18, 113.01, 111.85, 109.40 (CN), 104.78, 56.30 (CH), 55.21 (OCH_3), 55.13 (OCH_3), 20.93 (CH_3). **MS (ESI) *m/z*:** 502.8 $(M+1)^+$. **Elemental analysis for $C_{27}H_{23}N_3O_5S$:** C, 64.66; H, 4.62; N, 8.38; found: C, 64.35; H, 4.41; N, 8.15.

4.2.2.15. 2-amino-7-tosyl-4-(3,4,5-trimethoxyphenyl)-4,7-dihydropyrano[2,3-e]indole-3-carbonitrile (5o). White solid, Yield: 94%, M.P: 235–237 °C. **IR (υ_{max}/cm^{-1}):** 3322 (NH_2), 2182 (CN), 1174 (SO_2). **^{1}H NMR (300 MHz, DMSO)** δ = 7.84 (t, J = 6.1 Hz, 3H, Ar-H), 7.63 (d, J = 8.6 Hz, 1H, Ar-H), 7.35 (d, J = 8.2 Hz, 2H, Ar-H), 7.13–6.96 (m, 3H, Ar-H), 6.76 (d, J = 3.6 Hz, 1H, Ar-H), 6.51 (s, 2H, NH_2), 4.78 (s, 1H, CH), 3.69 (s, 6H, 2 × OCH_3), 3.61 (s, 3H, OCH_3), 2.29 (s, 3H, CH_3). **^{13}C NMR (75 MHz, DMSO)** δ = 160.05, 152.92, 145.76, 141.40, 140.65, 136.29, 133.93, 133.87, 130.28, 127.30, 126.74, 125.57, 120.41, 118.91, 116.83, 109.48 (CN), 104.74, 59.87 (OCH_3), 55.98 (CH), 55.75 (OCH_3), 20.96 (CH_3). **MS (ESI) *m/z*:** 532.5 $(M+1)^+$. **Elemental analysis for $C_{28}H_{25}N_3O_6S$:** C, 63.26; H, 4.74; N, 7.90; found: C, 63.07; H, 4.26; N, 7.75.

4.3. Biology

4.3.1. In-vitro cholinesterase activity

The AChE inhibition activity of test drugs and standards were determined using Ellman's method [34]. Standards and test drugs of six different concentrations of were prepared by diluting their stock solutions in sodium phosphate buffer (10 mM, pH 8.0). In 96-well plate, 20 μL test compound, 20 μL of AChE (0.2 U/mL) and 140 μL sodium phosphate buffer were mixed and incubated at RT for 15 min. Later, 5 mM acetylthiocholine iodide (ASCh) and 20 μL of 5 mM DTNB solution (containing 0.1% bovine serum albumin) (1:5) was added and the activity was determined spectrophotometrically at 412 nm every 60 *sec* intervals at 37 °C on Thermo Scientific Multiskan GO Microplate Spectrophotometer for 5 min. Percentage of inhibition was calculated by the following equation:

$$\text{Inhibition activity}(\%) = \frac{[A_{control} - A_{sample}]}{A_{control}} \text{x}100 \quad (1)$$

The IC_{50} values were determined graphically from inhibition curves (Inhibitor concentration vs Percent of inhibition) in triplicate using GraphPad Prism 5.0. Similarly, BuChE assay was performed using BuChE (0.25 U/mL) and butyrylthiocholine chloride (BTCh) as substrate.

4.3.2. Kinetic analysis of ChE inhibition

The inhibition mechanism of most active inhibitor **5o** was determined spectrophotometrically at 412 nm using by using Ellman's

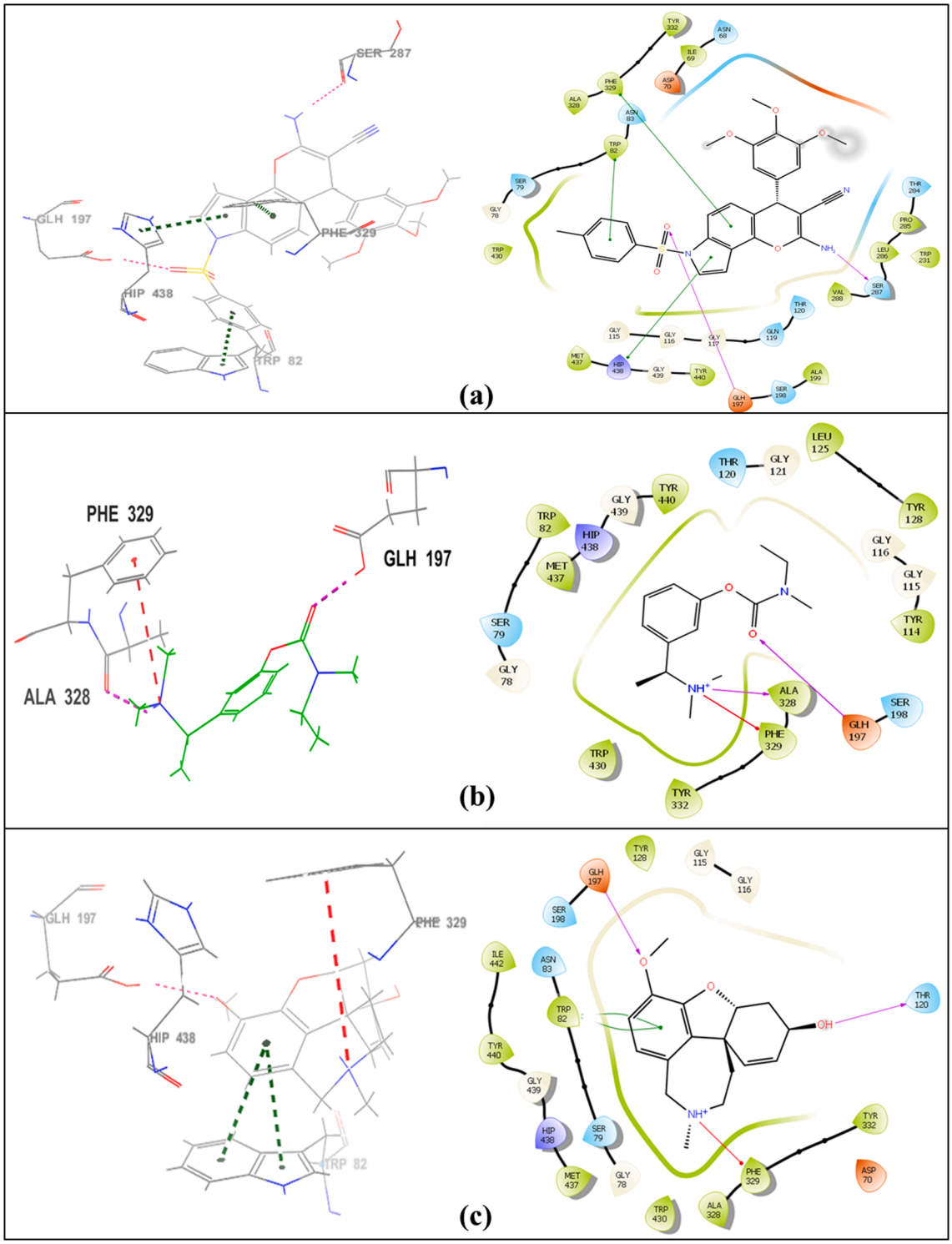

Fig. 7. 3D and 2D docking pose of (**a**) compound **5o**, (**b**) rivastigmine and (**c**) galantamine in the active site of BuChE.

method. For this purpose, five different concentrations of substrate (acetylthiocholine; 0.2, 0.25, 0.33, 0.5 and 1 mM) and three different concentrations of inhibitor (5, 10 and 20 μM) were used. Lineweaver-Burk plot of reciprocal rate of reaction (1/V) vs reciprocal of substrate (1/[S]) was constructed using GraphPad Prism 5.0 and the type of inhibition was determined. Also, Steady-state inhibition constant (K_i) was determined by plotting the Slopes versus the inhibitor concentration. Similar experiments were performed for BuChE using butyrylthiocholine as substrate. The experiments were performed in triplicate.

4.3.3. Determination of cell viability

Cytotoxicity was evaluated on N2a cells using (3-(4,5-dimethylthiazol-2-yl)-2,5-diphenyl tetrazolium bromide (MTT) assay. Briefly, in a 96-well plate N2a cells were seeded at a density of 5×10^3 cells per well containing Minimum Essential Medium Eagle (MEM) with 10% fetal bovine serum (FBS) and penicillin–streptomycin (50U/ml, 50 μg/ml) incubated at 37 °C under 5% CO_2. After incubation, the cells were treated with test compounds (20 μM and 40 μM in triplicate) and incubated under similar conditions for 24 h. Post incubation, 20 μL of

Table 4
ADME properties calculated by QikProp and PAINS alert of compounds **5(a-o)**.

Code	QP logPo/w[a]	QP logS[b]	QP logBB[c]	QP PCaco[d]	QP PMDCK[e]	% Human oral absorption[f]	Rule of five[g]	PAINS alert[h]
Acceptable Limit	−2.0 to 6.5	−6.5 to 0.5	−3 to 1.2	<25 to >500	<25 to >500	<25% to >80%		
5a	2.329	−6.322	−2.184	78.287	32.056	74.474	0	0
5b	3.733	−7.28	−1.694	171.327	74.91	88.782	0	0
5c	3.699	−7.312	−1.701	174.76	76.506	88.737	0	0
5d	3.704	−7.363	−1.713	176.071	77.21	88.825	0	0
5e	3.896	−7.683	−1.704	156.041	67.652	89.011	0	0
5f	4.104	−7.875	−1.467	177.066	191.601	91.21	0	0
5g	4.085	−7.863	−1.517	156.018	166.826	90.118	0	0
5h	3.838	−7.441	−1.486	175.997	139.532	89.606	0	0
5i	3.833	−7.511	−1.559	154.489	121.07	88.563	0	0
5j	2.866	−6.832	−2.25	52.589	20.876	74.524	0	0
5k	4.542	−8.376	−1.363	174.184	332.378	80.69	1	0
5l	2.845	−7.129	−2.573	32.039	12.221	70.552	0	0
5m	4.193	−8.153	−1.728	157.755	68.486	90.834	0	0
5n	3.871	−7.59	−1.831	166.283	72.496	76.403	1	0
5o	3.966	−7.684	−1.881	176.875	77.44	77.436	1	0

[a] Predicted octanol/water partition coefficient log P, [b] Predicted aqueous solubility; S in mol/L, [c] Predicted BBB permeability, [d] Predicted Caco-2 cell permeability in nm/s, [e] Predicted apparent MDCK cell permeability in nm/s, [f] Percentage of human oral absorption, [g] Number of violations of Lipinski's rule of five. [The rules are: mol MW < 500, QPlogPo/w < 5, donorHBB ≤ 5, acceptHB ≤ 10. Compounds that satisfy these rules are considered druglike. (The "five'' refers to the limits, which are multiples of 5)], [h] PAINS (Pan-assay interference compounds) alert.

MTT at a concentration of 0.5 mg/mL was added to the wells, and the plate was incubated for 4 h. The contents of the wells were gently discarded post incubation, without disturbing the cells. Thereafter, 100 μL of dimethyl sulfoxide (DMSO) was added to solubilise the formazan crystals. Plate was incubated for 30 min. The plate was then read at 570 nm with a microplate reader and cytotoxicity was calculated by considering absorbance of the control cells as 100% of the cell viability. Images were procured using Evos XL core system- AMEX1000.

4.3.4. Neuroprotective studies against H_2O_2-induced stress

The N2a cells were seeded into 96-well plates (5×10^3 cells/well) and allowed to adhere in a CO_2 incubator for 24 h. Cells were pre-treated with 20 μM and 40 μM of the test compounds and incubated for 2 h. After the incubation period, freshly prepared H_2O_2 (from 30% stock) was added at a concentration of 100 μM and left for an additional 24 h period. Thereafter, the cell viability was assessed using MTT assay (as stated earlier) to examine potential effects. Percentage protection against H_2O_2 was calculated by considering absorbance of the control cells as 100% of the cell viability.

4.3.5. DNA damage protection assay

DNA protection assay of compound **5o** was performed according to our previous report [39]. For this purpose, Fenton's reagent was prepared in ratio 1:1:1 using H_2O_2 (30 mM), ferric chloride (100 μM) and ascorbic acid (500 μM). The reaction mixture included 3 μL of pBR322 plasmid DNA (0.25 μg), 3 μL of compound (10, 20 and 50 μM), 2 μL of Fenton's reagent and 2 μL of nuclease free double distilled water. The reaction mixture was incubated on a waterbath at 37 °C for 30 min. After loading the mixture onto 1% agarose gel containing 20 μL of ethidium bromide (1 mg/ml), electrophoresis was performed. The results were visualized by viewing the gel under a BIORAD ChemiDoc MP imaging system.

4.4. Molecular docking

Glide (Maestro, version 8.5, Schrodinger, LLC, 2008) software was used to perform molecular docking studies. The crystal structure of AChE (PDB ID: 1EVE) and BuChE (PDB ID: 1P0I) were obtained from protein data bank. Docking experiments were conducted using Glide XP docking following the standard protocol and parameters [40].

4.5. Prediction of ADME properties

The ADME properties were calculated using QikProp in normal processing mode with default options.

4.6. PAINS

PAINS filter was evaluated using SwissADME [41].

Declaration of Competing Interest

The authors declare that they have no known competing financial interests or personal relationships that could have appeared to influence the work reported in this paper.

Acknowledgements

One of the authors (Sarfaraz Shaikh) is thankful to DST-PURSE, New Delhi for award of research fellowship. We are also thankful to Micro-analytical Laboratory, University of Mumbai for providing characterization facilities. The authors also thank Miss Heena Bhojwani and Miss Khushboo Begwani (K. M. Kundnani College of Pharmacy, Colaba, Mumbai, Maharashtra 400 005, India) for computer-aided drug design.

Appendix A. Supplementary data

Supplementary data to this article can be found online at https://doi.org/10.1016/j.bioorg.2021.104770.

References

[1] H.F. Kung, C.W. Lee, Z.P. Zhuang, M.P. Kung, C. Hou, K. Plössl, Novel stilbenes as probes for amyloid plaques, J. Am. Chem. Soc. 123 (2001) 12740–12741, https://doi.org/10.1021/ja0167147.
[2] M. Prince, A. Wimo, M. Guerchet, G.-C. Ali, Y.-T. Wu, M. Prina, World Alzheimer Report 2015, Alzheimer's Dis. Int. 13 (2015) 1-87. https://www.alz.co.uk/research/WorldAlzheimerReport2015.pdf.
[3] S. Singla, P. Piplani, Coumarin derivatives as potential inhibitors of acetylcholinesterase: synthesis, molecular docking and biological studies, Bioorg. Med. Chem. 24 (2016) 4587–4599, https://doi.org/10.1016/j.bmc.2016.07.061.
[4] W. Luo, Y. Chen, T. Wang, C. Hong, L.P. Chang, C.C. Chang, Y.C. Yang, S.Q. Xie, C. J. Wang, Design, synthesis and evaluation of novel 7-aminoalkyl-substituted flavonoid derivatives with improved cholinesterase inhibitory activities, Bioorg. Med. Chem. 24 (2016) 672–680, https://doi.org/10.1016/j.bmc.2015.12.031.
[5] C.J. Viau, R.D. Curren, K. Wallace, Cytotoxicity of tacrine and velnacrine metabolites in cultured rat, dog and human hepatocytes, Drug Cheimcal. Toxicol. 16 (1993) 227–239, https://doi.org/10.3109/01480549309081817.

[6] G. Kryger, I. Silman, J.L. Sussman, Structure of acetylcholinesterase complexed with E2020 (Aricept®): implications for the design of new anti-Alzheimer drugs, Structure 7 (1999) 297–307, https://doi.org/10.1016/S0969-2126(99)80040-9.
[7] P.K. Mukherjee, V. Kumar, M. Mal, P.J. Houghton, Acetylcholinesterase inhibitors from plants, Phytomedicine 14 (2007) 289–300, https://doi.org/10.1016/j.phymed.2007.02.002.
[8] N.A. Vyas, S.B. Singh, A.S. Kumbhar, D.S. Ranade, G.R. Walke, P.P. Kulkarni, V. Jani, U.B. Sonavane, R.R. Joshi, S. Rapole, Acetylcholinesterase and Aβ aggregation inhibition by heterometallic ruthenium(II)-platinum(II) polypyridyl complexes, Inorg. Chem. 57 (2018) 7524–7535, https://doi.org/10.1021/acs.inorgchem.8b00091.
[9] M.A.A. Radwan, E.A. Ragab, N.M. Sabry, S.M. El-Shenawy, Synthesis and biological evaluation of new 3-substituted indole derivatives as potential anti-inflammatory and analgesic agents, Bioorg. Med. Chem. 15 (2007) 3832–3841, https://doi.org/10.1016/j.bmc.2007.03.024.
[10] Y.M. Al-Hiari, A.M. Qaisi, M.M. El-Abadelah, W. Voelter, Synthesis and antibacterial activity of some substituted 3-(aryl)- and 3-(heteroaryl)indoles, Monatshefte Fur Chemie 137 (2006) 243–248, https://doi.org/10.1007/s00706-005-0424-6.
[11] O. Talaz, I. Gülçin, S. Göksu, N. Saracoglu, Antioxidant activity of 5,10-dihydroindeno[1,2-b]indoles containing substituents on dihydroindeno part, Bioorg. Med. Chem. 17 (2009) 6583–6589, https://doi.org/10.1016/j.bmc.2009.07.077.
[12] N. Karali, A. Gürsoy, F. Kandemirli, N. Shvets, F.B. Kaynak, S. Özbey, V. Kovalishyn, A. Dimoglo, Synthesis and structure-antituberculosis activity relationship of 1H-indole-2,3-dione derivatives, Bioorg. Med. Chem. 15 (2007) 5888–5904, https://doi.org/10.1016/j.bmc.2007.05.063.
[13] S. Battaglia, E. Boldrini, F. Da Settimo, G. Dondio, C. La Motta, A.M. Marini, G. Primofiore, Indole amide derivatives: Synthesis, structure-activity relationships and molecular modelling studies of a new series of histamine H1-receptor antagonists, Eur. J. Med. Chem. 34 (1999) 93–105, https://doi.org/10.1016/S0223-5234(99)80044-0.
[14] M.J.R.P. Queiroz, A.S. Abreu, M.S.D. Carvalho, P.M.T. Ferreira, N. Nazareth, M. São-José Nascimento, Synthesis of new heteroaryl and heteroannulated indoles from dehydrophenylalanines: antitumor evaluation, Bioorg. Med. Chem. 16 (2008) 5584–5589, https://doi.org/10.1016/j.bmc.2008.04.004.
[15] I. Denya, S.F. Malan, A.B. Enogieru, S.I. Omoruyi, O.E. Ekpo, E. Kapp, F.T. Zindo, J. Joubert, Design, synthesis and evaluation of indole derivatives as multifunctional agents against Alzheimer's disease, Medchemcomm. 9 (2018) 357–370, https://doi.org/10.1039/C7md00569E.
[16] M. Zheng, M. Zheng, D. Ye, Y. Deng, S. Qiu, X. Luo, K. Chen, H. Liu, H. Jiang, Indole derivatives as potent inhibitors of 5-lipoxygenase: design, synthesis, biological evaluation, and molecular modeling, Bioorg. Med. Chem. Lett. 17 (2007) 2414–2420, https://doi.org/10.1016/j.bmcl.2007.02.038.
[17] X. Song, A.M. Crider, S.F. Cruse, D. Ghosh, C. Klein-stevens, L. Liang, M. A. Scheideler, A. Varming, I. Søtofte, Cis- and trans-2,3,3a,4,5,9b-Hexahydro-1H-benz[e]indoles: synthesis and evaluation of dopamine D2 and D3 receptor binding affinity, Eur. J. Med. Chem. 34 (1999) 487–503, https://doi.org/10.1016/S0223-5234(99)80098-1.
[18] H. Takami, N. Kishibayashi, A. Ishii, T. Kumazawa, Indole and benzimidazole derivatives as steroid 5α-reductase inhibitors in the rat prostate, Bioorg. Med. Chem. 6 (1998) 2441–2448, https://doi.org/10.1016/S0968-0896(98)80018-7.
[19] N.K. Kaushik, N. Kaushik, P. Attri, N. Kumar, C.H. Kim, A.K. Verma, E.H. Choi, Biomedical importance of indoles, Molecules 18 (2013) 6620–6662, https://doi.org/10.3390/molecules18066620.
[20] N.R. Kamdar, D.D. Haveliwala, P.T. Mistry, S.K. Patel, Synthesis and evaluation of in vitro antitubercular activity and antimicrobial activity of some novel 4H-chromeno[2,3-d] pyrimidine via 2-amino-4-phenyl-4H-chromene-3-carbonitriles, Med. Chem. Res. 20 (2011) 854–864, https://doi.org/10.1007/s00044-010-9399-x.
[21] J. Mori, M. Iwashima, M. Takeuchi, H. Saito, A synthetic study on antiviral and antioxidative chromene derivative, Chem. Pharm. Bull. 54 (2006) 391–396, https://doi.org/10.1248/cpb.54.391.
[22] L. Piazzi, A. Rampa, A. Bisi, S. Gobbi, F. Belluti, A. Cavalli, M. Bartolini, V. Andrisano, P. Valenti, M. Recanatini, 3-(4-{[Benzyl(methyl)amino]methyl}-phenyl)-6,7-dimethoxy-2H-2-chromenone (AP2238) inhibits both acetylcholinesterase and acetylcholinesterase-induced β-amyloid aggregation: a dual function lead for Alzheimer's disease therapy, J. Med. Chem. 46 (2003) 2279–2282, https://doi.org/10.1021/jm0340602.
[23] Z. Chen, W. Xu, K. Liu, S. Yang, H. Fan, P.S. Bhadury, D.Y. Hu, Y. Zhang, Synthesis and antiviral activity of 5-(4-chlorophenyl)-1,3,4- thiadiazole sulfonamides, Molecules 15 (2010) 9046–9056, https://doi.org/10.3390/molecules15129046.
[24] A.P. Keche, G.D. Hatnapure, R.H. Tale, A.H. Rodge, S.S. Birajdar, V.M. Kamble, A novel pyrimidine derivatives with aryl urea, thiourea and sulfonamide moieties: synthesis, anti-inflammatory and antimicrobial evaluation, Bioorg. Med. Chem. Lett. 22 (2012) 3445–3448, https://doi.org/10.1016/j.bmcl.2012.03.092.
[25] R. Sharma, S.S. Soman, Design and synthesis of sulfonamide derivatives of pyrrolidine and piperidine as anti-diabetic agents, Eur. J. Med. Chem. 90 (2015) 342–350, https://doi.org/10.1016/j.ejmech.2014.11.041.
[26] N. Masand, S.P. Gupta, R.L. Khosa, N-substituted aryl sulphonamides as potential anti-Alzheimer's agents: design, synthesis and biological evaluation, Curr. Comput. Aided. Drug Des. 14 (2018) 338–348, https://doi.org/10.2174/1573409914666180604115425.
[27] B. López-Iglesias, C. Pérez, J.A. Morales-García, S. Alonso-Gil, A. Pérez-Castillo, A. Romero, M.G. López, M. Villarroya, S. Conde, M.I. Rodríguez-Franco, New melatonin- N, N -dibenzyl(N -methyl)amine hybrids: potent neurogenic agents with antioxidant, cholinergic, and neuroprotective properties as innovative drugs for alzheimer's disease, J. Med. Chem. 57 (2014) 3773–3785, https://doi.org/10.1021/jm5000613.
[28] A. Więckowska, M. Kołaczkowski, A. Bucki, J. Godyń, M. Marcinkowska, K. Więckowski, P. Zaręba, A. Siwek, G. Kazek, M. Głuch-Lutwin, P. Mierzejewski, P. Bienkowski, H. Sienkiewicz-Jarosz, D. Knez, T. Wichur, S. Gobec, B. Malawska, Novel multi-target-directed ligands for Alzheimer's disease: combining cholinesterase inhibitors and 5-HT6 receptor antagonists. Design, synthesis and biological evaluation, Eur. J. Med. Chem. 124 (2016) 63–81, https://doi.org/10.1016/j.ejmech.2016.08.016.
[29] S. Ghanei-Nasab, M. Khoobi, F. Hadizadeh, A. Marjani, A. Moradi, H. Nadri, S. Emami, A. Foroumadi, A. Shafiee, Synthesis and anticholinesterase activity of coumarin-3-carboxamides bearing tryptamine moiety, Eur. J. Med. Chem. 121 (2016) 40–46, https://doi.org/10.1016/j.ejmech.2016.05.014.
[30] R.S. Kumar, A.I. Almansour, N. Arumugam, D.M. Al-thamili, A. Basiri, D. Kotresha, T.S. Manohar, S. Venketesh, M. Asad, A.M. Asiri, Highly functionalized 2-amino-4H-pyrans as potent cholinesterase inhibitors, Bioorg. Chem. 81 (2018) 134–143, https://doi.org/10.1016/j.bioorg.2018.08.009.
[31] H. Boulebd, L. Ismaili, M. Bartolini, A. Bouraiou, V. Andrisano, H. Martin, A. Bonet, I. Moraleda, I. Iriepa, M. Chioua, A. Belfaitah, J. Marco-Contelles, Imidazopyranotacrines as non-hepatotoxic, selective acetylcholinesterase inhibitors, and antioxidant agents for Alzheimer's disease therapy, Molecules 21 (2016) 1–16, https://doi.org/10.3390/molecules21040400.
[32] R. Swetha, D. Kumar, S.K. Gupta, A. Ganeshpurkar, R. Singh, G. Gutti, D. Kumar, S. Jana, S. Krishnamurthy, S.K. Singh, Multifunctional hybrid sulfonamides as novel therapeutic agents for Alzheimer's disease, Future Med. Chem. 11 (2019) 3161–3177, https://doi.org/10.4155/fmc-2019-0106.
[33] Y. Wada, Y. Harayama, D. Kamimura, M. Yoshida, T. Shibata, K. Fujiwara, K. Morimoto, H. Fujioka, Y. Kita, The synthetic and biological studies of discorhabdins and related compounds, Org. Biomol. Chem. 9 (2011) 4959–4976, https://doi.org/10.1039/c1ob05058c.
[34] G.L. Ellman, K.D. Courtney, V. Andres, R.M. Featherstone, A new and rapid colorimetric determination of acetylcholinesterase activity, Biochem. Pharmacol. 7 (1961) 88–95, https://doi.org/10.1016/0006-2952(61)90145-9.
[35] I. Gulcin, M.E. Buyukokuroglu, O.I. Kufrevioglu, Metal chelating and hydrogen peroxide scavenging effects of melatonin, J. Pineal Res. 34 (2003) 278–281, https://doi.org/10.1034/j.1600-079X.2003.00042.x.
[36] M.P. Jorge, C. Madjarof, A.L.T.G. Ruiz, A.T. Fernandes, R.A.F. Rodrigues, I.M. de Oliveira Sousa, M.A. Foglio, J.E. de Carvalho, Evaluation of wound healing properties of Arrabidaea chica Verlot extract, J. Ethnopharmacol. 118 (2008) 361–366, https://doi.org/10.1016/j.jep.2008.04.024.
[37] W.R. Markesbery, Oxidative stress hypothesis in Alzheimer's disease, Free Radic. Biol. Med. 23 (1997) 134–147, https://doi.org/10.1016/S0891-5849(96)00629-6.
[38] J.B. Baell, G.A. Holloway, New substructure filters for removal of pan assay interference compounds (PAINS) from screening libraries and for their exclusion in bioassays, J. Med. Chem. 53 (2010) 2719–2740, https://doi.org/10.1021/jm901137j.
[39] S. Shaikh, P. Dhavan, G. Pavale, M.M.V. Ramana, B.L. Jadhav, Design, synthesis and evaluation of pyrazole bearing α-aminophosphonate derivatives as potential acetylcholinesterase inhibitors against Alzheimer's disease, Bioorg. Chem. 96 (2020) 103589, https://doi.org/10.1016/j.bioorg.2020.103589.
[40] A.J. Joshi, H.R. Bhojwani, U.J. Joshi, Strategies to select the best pharmacophore model: a case study in pyrazoloquinazoline class of PLK-1 inhibitors, Med. Chem. Res. 27 (2018) 234–260, https://doi.org/10.1007/s00044-017-2057-9.
[41] A. Grosdidier, V. Zoete, O. Michielin, SwissDock, a protein-small molecule docking web service based on EADock DSS, Nucleic Acids Res. 39 (2011) 270–277, https://doi.org/10.1093/nar/gkr366.